
An OpenMind for 3D medical vision self-supervised learning

Tassilo Wald^{*1234} Constantin Ulrich^{*156} Jonathan Suprijadi⁷ Michal Nohel⁷⁸⁹ Robin Peretzke¹⁵
Klaus H. Maier-Hein¹²³⁴¹⁰

Abstract

The field of 3D medical vision self-supervised learning lacks consistency and standardization. While many methods have been developed it is impossible to identify the current state-of-the-art, due to i) varying and small pre-training datasets, ii) varying architectures, and iii) being evaluated on differing downstream datasets. In this paper we bring clarity to this field and lay the foundation for further method advancements: We a) publish the largest publicly available pre-training dataset comprising 114k 3D brain MRI volumes and b) benchmark existing SSL methods under common architectures and c) provide the code of our framework publicly to facilitate rapid adoption and reproduction.

This pre-print *only describes* the dataset contribution (a); Data, benchmark, and codebase will be made available shortly.

1. Introduction

Self-Supervised Learning (SSL) has emerged as a transformative approach in deep learning, enabling the extraction of robust and general representations from data-rich domains Assran et al. (2023); Oquab et al. (2023); He et al. (2022). This paradigm has led to significant advancements in areas with abundant data, such as natural language processing and natural image computer vision. However, the adoption of

SSL within 3D medical image computing remains limited.

Currently, the field predominantly follows two approaches to develop vision models: training models from scratch, often using the nnU-Net framework (Isensee et al., 2021), or adopting supervised pre-training with large, monolithic annotated datasets (Wasserthal et al., 2023; Qu et al., 2024; Huang et al., 2023) or aggregates of smaller datasets to increase scale ?. While the latter approach indicates a willingness to adopt pre-training paradigms, they also highlight the underutilization of self-supervised learning in 3D medical imaging.

We believe this lack of SSL method development and adoption can be attributed to two major factors:

1) A lack of a sufficiently large, open-source 3D dataset that can be used out of the box for pre-training. Currently, acquiring large unlabeled datasets for pre-training is a non-trivial task. While large studies like the UK-BioBank or the NIH Adolescent Brain Cognitive Development (ABCD) exist and hold >100k or >40k 3D Volumes respectively, access hinges on an internal review process necessitating an appropriate project proposal. UK-BioBank even comes with a fee to use the data and can no longer be downloaded as of recently.

Hence, the majority of current SSL methods are either developed on large, restricted or proprietary datasets (Wald et al., 2024; Wang et al., 2023; Munk et al., 2024; Zhang et al., 2024) or are developed on small-scale publicly available datasets (Chen et al., 2023; Zhuang et al., 2023; He et al., 2023; Zhou et al., 2021; Wu et al., 2024; Tang et al., 2022; 2024).

To add to the complexity, datasets are often subject to unique Data Usage Agreements (DUAs) that impose varying levels of restrictions on recipients. These rules may include: (i) mandatory acknowledgments, (ii) internal administrative review of manuscripts prior to submission (OASIS, 2024; PPML, 2024; ADNI, 2024; MCSA, 2024; HABS-HD, 2024), (iii) inclusion of a consortium in the author list (ADNI, 2024; MCSA, 2024; HABS-HD, 2024), or (iv) requiring the dataset’s name to appear in the manuscript title (MCSA, 2024). While mandatory acknowledgments are reasonable and widely accepted, the other requirements can impose

^{*}Equal contribution ¹Division of Medical Image Computing, German Cancer Research Center (DKFZ), Heidelberg, Germany ²Faculty of Mathematics and Computer Science, University of Heidelberg, Germany ³Helmholtz Foundation Model Initiative, Helmholtz, Germany ⁴Helmholtz Imaging, DKFZ, Germany ⁵Medical Faculty Heidelberg, University of Heidelberg, Germany ⁶National Center for Tumor Diseases (NCT), Heidelberg ⁷Work done while at DKFZ. ⁸Department of Biomedical Engineering, Faculty of Electrical Engineering and Communication, Brno University of Technology, Czech Republic ⁹University hospital Ostrava, Department of Deputy director for science, research and education ¹⁰Pattern Analysis and Learning Group, Department of Radiation Oncology. Correspondence to: Tassilo Wald <tassilo.wald@dkfz-heidelberg.de>.

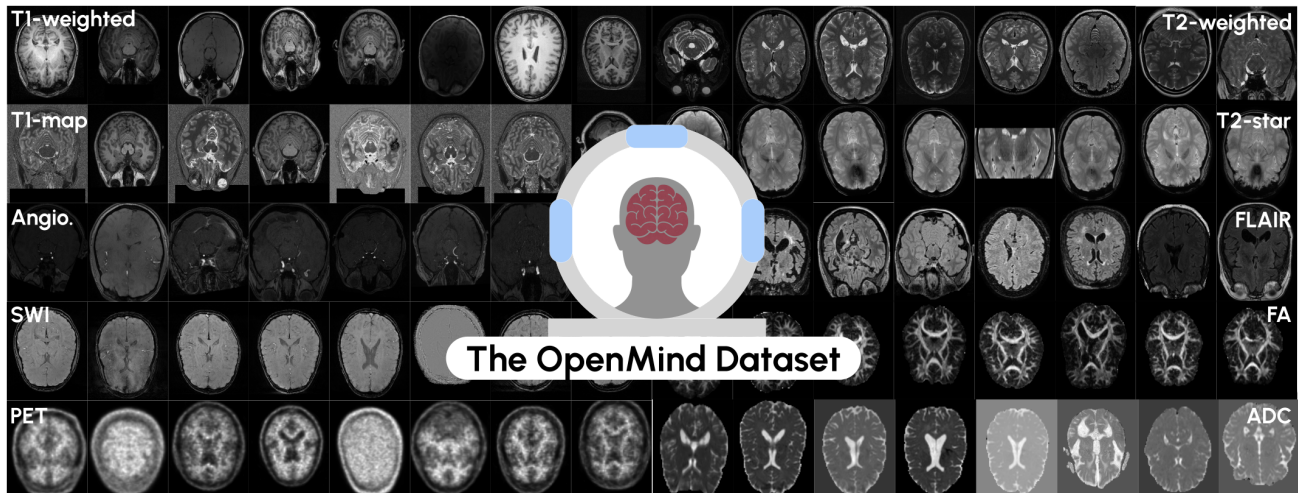


Figure 1. The OpenMind dataset contains 114k 3D brain volumes of 23 different modalities. It represents the largest openly accessible dataset of 3D medical images currently available.

significant burdens on researchers by introducing unnecessary barriers to the aggregation of large, unlabeled datasets for SSL method development. This, in turn, contributes to a fragmented landscape of pre-training methods that are difficult to compare due to variations in the underlying pre-training data.

2) A lack of comparability disallowing identification of the best method: In order to adopt either existing models or conduct one’s own pre-training it is important to know which model or pre-training method is the best. Currently, this is an impossible task, due to i) different pre-training dataset selection (as previously highlighted) ii) some methods using CNNs for pre-training (Wald et al., 2024; Zhou et al., 2021; Munk et al., 2024; Zhang et al., 2024), some ViT-like Transformers (Chen et al., 2023; Zhuang et al., 2023), other Swin Transformers (Tang et al., 2022; Wu et al., 2024) and even others hybrid architectures (Tang et al., 2024; Wang et al., 2023). Orthogonally to this most methods diverge strongly in their downstream fine-tuning dataset making comparisons between methods even more complicated.

To address these issues we provide i) the largest publicly available 3D dataset, comprising 114k 3D volumes of 23 different brain MRI modalities and ii) conduct a comprehensive self-supervised learning benchmark on this pre-training dataset and evaluate, current state-of-the-art CNN and transformer-based architectures. Moreover, we iii) open-source our pre-training framework to enable rapid reproduction and extension of the current SSL methods for 3D medical image segmentation.

Table 1. Large medical datasets are restricted through custom DUAs limiting overall applicability. E.g. ADNI requires co-authorship and a review of a paper prior to submission. The OpenMind dataset represents the largest open dataset to-date.

| Dataset | # Patients | # 3D Volumes | # Modalities | Access |
|-----------------|---------------|----------------|--------------|------------------|
| ABCD | 11,385 | 41,580 | 2 | Restricted |
| PPMI | 2,011 | 9,554 | 5 | Restricted |
| ADNI | 1,563 | 9,548 | 3 | Restricted |
| OASIS3 | 1,376 | 15,872 | 7 | Restricted |
| OASIS4 | 661 | 4,021 | 5 | Restricted |
| BraTS21 | 1,251 | 5,004 | 4 | CC-BY-4.0 |
| CT-RATE | 21,304 | 50,188 | 2 | CC-BY-NC-4.0 |
| OpenMind | 34,191 | 114,570 | 23 | CC-BY-4.0 |

2. The OpenMind Dataset

Accessing large-scale open datasets for self-supervised learning (SSL) in the 3D medical imaging domain poses significant challenges. Many datasets require application processes, review board approvals, or even usage fees, hindering the advancement of SSL methodologies.

To address this gap, we introduce the OpenMind dataset: a large-scale, one-click downloadable resource containing over 114k head-and-neck MRI volumes across various modalities, sourced from the OpenNeuro platform. OpenMind is the largest freely accessible 3D brain imaging dataset to date, surpassing the NIH Adolescent Brain Cognitive Decline initiative by a factor of three. Crucially, it is published under a CC-BY license, ensuring unrestricted use (see Table 1).

2.1. Dataset creation

All the data was sourced or derived from datasets available on the OpenNeuro platform. OpenNeuro (formerly known as openfMRI) is a publicly accessible data repository designed to support neurological research, adhering to the FAIR principles (Findable, Accessible, Interoperable, Reusable). The platform currently hosts over 1,200 public datasets, encompassing data from more than 51,300 participants. Due to the diverse nature of its collection, OpenNeuro includes a wide array of imaging modalities, such as MRI, PET, fMRI, MEG, EEG, and iEEG, from studies involving both healthy and diseased participants, enabling research across various aspects of neurology.

From this extensive collection, all available 3D MRIs, such as T1-weighted and T2-weighted scans, as well as 4D diffusion-weighted MRIs were collected from about 700 different studies. This aggregation resulted in a total of 71k 3D MRI¹ scans and 15k 4D diffusion-weighted images from a total of 34,191 participants. While the 71k 3D MRI scans, encompassing various imaging modalities, can be directly utilized by existing 3D self-supervised learning (SSL) methods, the 4D diffusion-weighted images require pre-processing before being compatible with these approaches.

Overall, due to the high amount of independent studies, the OpenMind dataset provides unprecedented levels of diversity regarding participant age distribution, countries of origin, MRI modalities, scanner manufacturer, model and scanning protocols.

DWI Preprocessing Diffusion-weighted imaging (DWI) is an advanced MRI modality that captures the diffusion of water molecules within tissue across 3D space, often guided by varying magnetic gradient fields to measure directional diffusion. This technique provides crucial insights into tissue microstructure and is widely used for detecting abnormalities such as strokes, tumors, and white matter changes. In clinical and research settings, DWI data are often pre-processed into more interpretable 3D derivatives, including apparent diffusion coefficient (ADC) maps, and fractional anisotropy (FA) maps, which simplify analysis and interpretation. Additionally, T2-weighted images can often be derived from DWI scans. To harness the rich information within DWI data for our study, we pre-processed the images into ADC maps, FA maps, and T2-weighted images, resulting in an additional 43k 3D images. The detailed pre-processing pipeline is described in Appendix A.

Defacing With these 114k 3D images, self-supervised pre-training becomes feasible. However, due to the nature of these scans capturing the head-and-neck region, many structural images have undergone an anonymization pro-

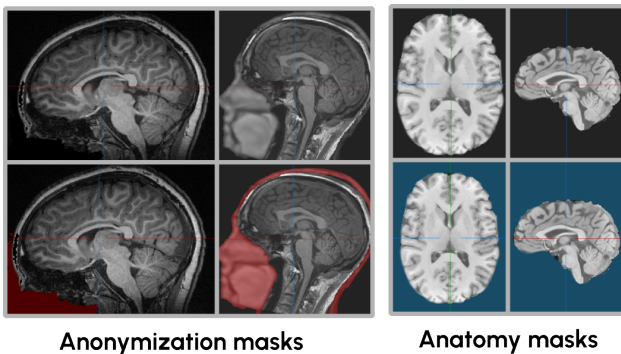


Figure 2. Structural images are often defaced, have the face blurred or have been brain-extracted to assure the privacy of the participants, which can potentially harm reconstruction based SSL methods. Anonymization and anatomy masks are provided to allow taking this into account during method development.

cess to ensure participant privacy. Common anonymization techniques include defacing, blurring of everything but the brain or brain extraction, see Figure 2. These augmented regions can interfere with reconstruction-based SSL methods, potentially penalizing models for attempting to reconstruct plausible anatomical features in anonymized regions. To allow taking these regions into account complementary masks to the images are mandatory. Unfortunately, not all of the 700 datasets provide these masks, despite applying some sort of anonymization. To address this issue, we generate associated anonymization masks and anatomy masks for cases where these are not provided (Figure 2 bottom). The anonymization mask identifies areas where anatomical structures have been artificially modified or removed and where no loss should be calculated, whereas anatomy masks indicate where relevant foreground is present allowing to avoid sampling non-empty patches which may speed up the convergence of the pre-training methods. Both of these masks are created using a recently published defacing and anonymization tool².

Meta-Data enrichment While OpenNeuro follows the Brain Imaging Data Structure (BIDS) format, metadata organization varies significantly across datasets. Participant demographics (e.g., age, sex, health status) and image acquisition details (e.g., repetition times, scanner types, imaging protocols) are inconsistently reported, creating challenges for systematic analysis.

We curated and harmonized this disparate metadata into a unified, complementary metadata structure. This standardized framework ensures consistency and enables users to efficiently filter the OpenMind dataset based on specific

¹This includes a minority of 653 PET scans.

²Code available here.

selection criteria, such as participant characteristics or imaging parameters. This process enhances the accessibility and usability of the dataset, making it easier for researchers to identify and extract relevant data subsets.

In addition to the existing metadata, an *image quality score* is provided for each imaging modality across the 700 datasets. This score is designed to evaluate the usability of the images for self-supervised learning (SSL) pre-training. The assessment considers factors such as noise levels, motion artifacts, and other potentially quality-degrading elements, condensing these evaluations into a unified score ranging from 1 to 5. The quality scores were determined through the manual inspection of multiple images from each modality in each dataset, conducted independently by two raters to ensure reliability.

Together with the harmonized metadata, this unified set of quality scores aims to facilitate the development of data-centric techniques for 3D medical imaging, an area still in its early stages due to the limited availability of large-scale, high-quality datasets. By addressing this gap, the dataset encourages innovation and progress in pre-training methodologies for medical imaging research.

Useability To lower the barrier to entry, we share all 114k 3D images on Hugging Face together with associated anonymization and anatomy masks and harmonized metadata. The associated repository will be made available on [Hugging Face](#) once the benchmarking concludes³.

References

- ADNI. Alzheimer’s disease neuroimaging initiative data use agreement, 2024. URL <https://ida.loni.usc.edu/collaboration/access/appApply.jsp?project=ADNI>.
- Assran, M., Duval, Q., Misra, I., Bojanowski, P., Vincent, P., Rabat, M., LeCun, Y., and Ballas, N. Self-supervised learning from images with a joint-embedding predictive architecture. In *Proceedings of the IEEE/CVF Conference on Computer Vision and Pattern Recognition*, pp. 15619–15629, 2023.
- Chen, Z., Agarwal, D., Aggarwal, K., Safta, W., Balan, M. M., and Brown, K. Masked image modeling advances 3d medical image analysis. In *Proceedings of the IEEE/CVF Winter Conference on Applications of Computer Vision*, pp. 1970–1980, 2023.
- HABS-HD. Health and aging brain study: Health disparities data use agreement, 2024. URL https://ida.loni.usc.edu/collaboration/access/appApply.jsp?project=HABS_HD.
- He, K., Chen, X., Xie, S., Li, Y., Dollár, P., and Girshick, R. Masked autoencoders are scalable vision learners. In *Proceedings of the IEEE/CVF conference on computer vision and pattern recognition*, pp. 16000–16009, 2022.
- He, Y., Yang, G., Ge, R., Chen, Y., Coatrieux, J.-L., Wang, B., and Li, S. Geometric visual similarity learning in 3d medical image self-supervised pre-training. In *Proceedings of the IEEE/CVF Conference on Computer Vision and Pattern Recognition*, pp. 9538–9547, 2023.
- Huang, Z., Wang, H., Deng, Z., Ye, J., Su, Y., Sun, H., He, J., Gu, Y., Gu, L., Zhang, S., et al. Stu-net: Scalable and transferable medical image segmentation models empowered by large-scale supervised pre-training. *arXiv preprint arXiv:2304.06716*, 2023.
- Isensee, F., Jaeger, P. F., Kohl, S. A., Petersen, J., and Maier-Hein, K. H. nnu-net: a self-configuring method for deep learning-based biomedical image segmentation. *Nature methods*, 18(2):203–211, 2021.
- MCSA. Mayo clinic study of aging data use agreement, 2024. URL <https://ida.loni.usc.edu/collaboration/access/appApply.jsp?project=MCSA>.
- Munk, A., Amsdorf, J., Llambias, S., and Nielsen, M. Amaes: Augmented masked autoencoder pretraining on public brain mri data for 3d-native segmentation. *arXiv preprint arXiv:2408.00640*, 2024.
- OASIS. Open access series of imaging studies data use agreement, 2024. URL <https://sites.wustl.edu/oasisbrains/>.
- Oquab, M., Darcet, T., Moutakanni, T., Vo, H., Szafraniec, M., Khalidov, V., Fernandez, P., Haziza, D., Massa, F., El-Nouby, A., et al. Dinov2: Learning robust visual features without supervision. *arXiv preprint arXiv:2304.07193*, 2023.
- PPMI. Parkinson’s progression markers initiative data use agreement, 2024. URL <https://ida.loni.usc.edu/collaboration/access/appApply.jsp?project=PPMI>.
- Qu, C., Zhang, T., Qiao, H., Tang, Y., Yuille, A. L., Zhou, Z., et al. Abdomenatlas-8k: Annotating 8,000 ct volumes for multi-organ segmentation in three weeks. *Advances in Neural Information Processing Systems*, 36, 2024.
- Tang, F., Xu, R., Yao, Q., Fu, X., Quan, Q., Zhu, H., Liu, Z., and Zhou, S. K. Hypspark: Hybrid sparse masking for large scale medical image pre-training. *arXiv preprint arXiv:2408.05815*, 2024.

³This will be at latest mid March 2025.

- Tang, Y., Yang, D., Li, W., Roth, H. R., Landman, B., Xu, D., Nath, V., and Hatamizadeh, A. Self-supervised pre-training of swin transformers for 3d medical image analysis. In *Proceedings of the IEEE/CVF conference on computer vision and pattern recognition*, pp. 20730–20740, 2022.
- Wald, T., Ulrich, C., Lukyanenko, S., Goncharov, A., Paderno, A., Maerkisch, L., Jaeger, P. F., and Maier-Hein, K. Revisiting mae pre-training for 3d medical image segmentation. *arXiv preprint arXiv:2410.23132*, 2024.
- Wang, G., Wu, J., Luo, X., Liu, X., Li, K., and Zhang, S. Mis-fm: 3d medical image segmentation using foundation models pretrained on a large-scale unannotated dataset. *arXiv preprint arXiv:2306.16925*, 2023.
- Wasserthal, J., Breit, H.-C., Meyer, M. T., Pradella, M., Hinck, D., Sauter, A. W., Heye, T., Boll, D. T., Cyriac, J., Yang, S., et al. Totalsegmentator: robust segmentation of 104 anatomic structures in ct images. *Radiology: Artificial Intelligence*, 5(5), 2023.
- Wu, L., Zhuang, J., and Chen, H. Voco: A simple-yet-effective volume contrastive learning framework for 3d medical image analysis. In *Proceedings of the IEEE/CVF Conference on Computer Vision and Pattern Recognition*, pp. 22873–22882, 2024.
- Zhang, X., Wu, Y., Angelini, E., Li, A., Guo, J., Rasmussen, J. M., O’Connor, T. G., Wadhwa, P. D., Jackowski, A. P., Li, H., Posner, J., Laine, A. F., and Wang, Y. Mapseg: Unified unsupervised domain adaptation for heterogeneous medical image segmentation based on 3d masked autoencoding and pseudo-labeling, 2024.
- Zhou, Z., Sodha, V., Pang, J., Gotway, M. B., and Liang, J. Models genesis. *Medical image analysis*, 67:101840, 2021.
- Zhuang, J.-X., Luo, L., and Chen, H. Advancing volumetric medical image segmentation via global-local masked autoencoder. *arXiv preprint arXiv:2306.08913*, 2023.

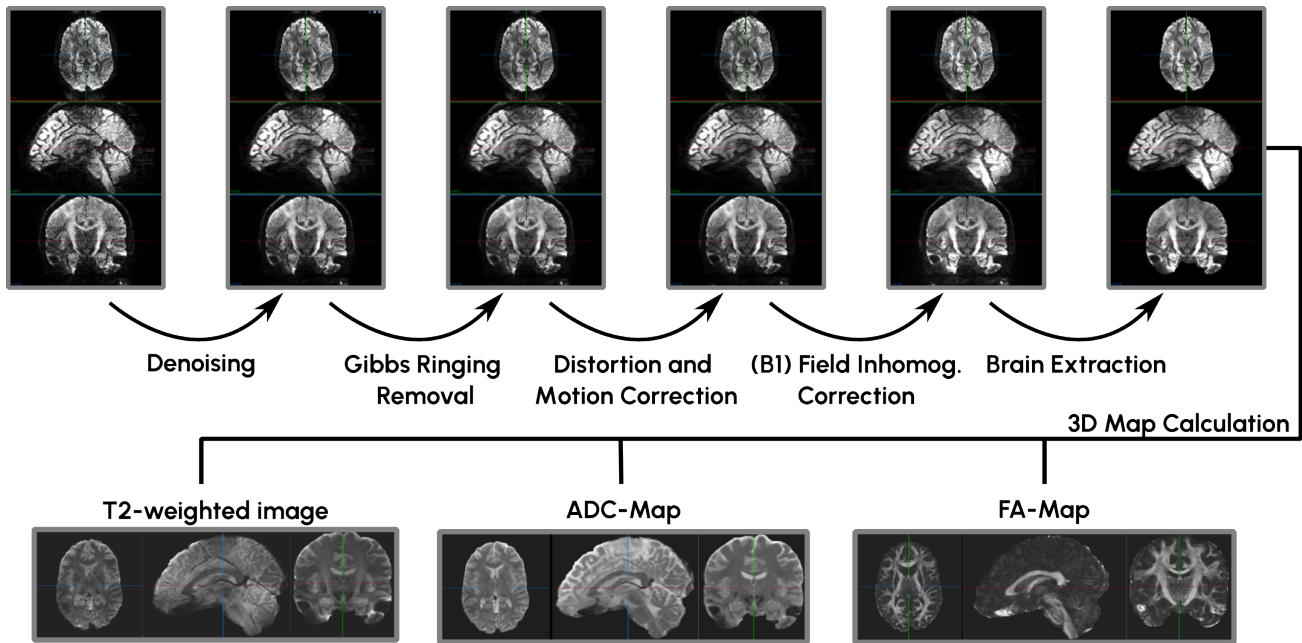


Figure 3. **DWI preprocessing pipeline:** To derive 3D images from the 4D DWI images, they are processed through six steps, denoising, ringing removal, co-registration, field correction, brain extraction, and lastly 3D derivative creation. Best viewed on a screen to see the differences between steps.

A. DWI Preprocessing

Diffusion-weighted imaging (DWI) measures the diffusion of water molecules in tissue across 3D space. The direction of this diffusion process can be influenced by applying additional magnetic field gradients, allowing researchers to identify tissues that are more or less permeable to water diffusion in specific directions. Because the diffusion process is directionally dependent, multiple images are acquired using gradients of varying strengths to, for example, quantify anisotropies in diffusion behavior. As a result, DWIs are typically composed of a stack of 3D images, forming complex 4D images that are challenging to process and integrate.

To manage the complexity of these 4D images, they are preprocessed into more manageable single 3D image formats that describe specific properties derived from the diffusion measurements in a more interpretable manner. These 3D derivatives of the DWIs allow easier integration into standard SSL pipelines. Specifically, we create T2-weighted, ADC, and FA maps from the original 4D DWI stacks.

The overall preprocessing pipeline is composed of six steps, displayed in Figure 3: i) Denoising of each 3D image. ii) Gibbs ringing artifact removal of each 3D image. iii) Co-registration of all images to one reference image to correct for potential distortions and motion artifacts. iv) Field correction of potential B1 field inhomogeneities. v) Brain extraction to remove skull and potentially existing face tissue that is not accounted for in the Map creation. vi) Actual creation of the 3D derivatives, namely a T2-weighted image, an ADC-Map and an FA-Map.